OPTICAL SCIENCES CENTER

TECHNICAL REPORT 64

PROPERTIES OF GENERALIZED BENDING

James H. Darnauer

28 February 1971

PROPERTIES OF GENERALIZED BENDING

James H. Darnauer

Optical Sciences Center
The University of Arizona
Tucson, Arizona 85721
28 February 1971

FOREWORD

This technical report is adapted from a thesis submitted in partial fulfillment of the requirements for the degree of Master of Science in Optical Sciences at the University of Arizona.

The thesis was completed and approved in August 1970 .

ABSTRACT

Generalized bending is a one-parameter family of changes to two curvatures and related thicknesses of a previously defined optical system consisting of spherical and plane refracting surfaces. This family of changes leaves first-order properties invariant at all other surfaces in the system. Thus, third-order aberrations at the other surfaces are also unchanged. The third-order aberrations may then be expressed as functions of independent generalized bends at different locations; therefore, simultaneous correction of several aberrations is possible.

Comparison of ray fan plots for real rays through an optical system shows marked differences for various degrees and locations of generalized bending. Surfaces at which a generalized bend would make significant changes to aberrations of the original lens are easily identified. This use of generalized bending would be helpful in advanced stages of a design routine.

CONTENTS

CHAPTER I

INTRODUCTION

The aberrations of a simple, positive, thin lens, which are related to changes in the shape or bending of the simple lens, are discussed in most texts concerning geometrical optics such as Jenkins and White (1957). But it is not easy to state the relationship between aberrations and the shape of a thick, real element buried in the middle of a compound optical system. One cannot make a simple change in the shape of one element without changing all of the properties of that system. On the other hand, generalized bending permits a relatively simple alteration of an arbitrary pair of adjacent surfaces while retaining the previous first-order quantities at all other surfaces and consequently maintaining the third-order aberration contribution of all other surfaces as well.

The generalized bending equations of Sutton (1963), their derivation, their properties, and their possible value and application to optical design are presented below. The sign convention and notation used in this derivation and throughout the rest of this paper will agree essentially with *MIL-HDBK-141* (Hopkins and Hanau, 1962, pp. 5-4, 5-5, and 5-32).

Light is considered to be traveling from left to right from an object surface through a consecutively numbered series of surfaces to an image plane. We assume a right-hand coordinate system with the optical axis of the system along the Z-axis and with positive Z-direction to the right. The Y-Z plane will be the meridional plane with positive Y-direction upward. Normally, object points will be picked to have a negative Y value in an X-Y plane so that the image height produced by a normal focal system will be positive. A general surface will be called the jth surface. The curvature of the jth surface, c_j, is equal to the reciprocal of the radius of curvature of the surface, r_j. Both are positive if the center of curvature is to the right and negative if it is to the left. The distance, referred to as thickness t_j, along the axis from the jth to the j+1 surface is positive if the j+1 surface lies to the right of the jth surface, and it is negative if it lies to the left. The refractive index between the jth and j+1 surface is n_j. The heights of axial and oblique rays at the jth surface are Y_j and $\overline{Y}_j$, respectively. Lowercase letters y_j and $\overline{y}_j$ represent the paraxial heights of the marginal and chief ray, respectively. The slope angles of the marginal and chief rays in the space between the jth and j+1 surfaces are u_j and $\overline{u}_j$, respectively. The angles are equal to $(y_{j+1} - y_j)/t_j$ and $(\overline{y}_{j+1} - \overline{y}_j)/t_j$ and retain the algebraic sign of these quantities.

In this derivation it is assumed that an optical system exists for which curvatures, thicknesses, and refractive indices are known. We will consider three consecutive surfaces (Fig. 1) numbered 1, 2, and 3 to represent any three consecutive surfaces of an optical system. We desire to find a one-parameter family of values for c_1, t_1, c_2, and t_2 for which the paraxial quantities at the third surface, u_2, y_3, $\overline{u}_2$, and $\overline{y}_3$, remain invariant for a given set of input values u_0, y_1, $\overline{u}_0$, and $\overline{y}_1$. First, using paraxial refraction and transfer equations, u_2 and $\overline{u}_2$ are written in terms of u_0, y_1, $\overline{u}_0$, $\overline{y}_1$, c_1, t_1, and c_2. Then c_1, t_1, and c_2 are given new values, c_1^*, t_1^*, and c_2^*, which would imply new values u_2^* and $\overline{u}_2^*$. Since we demand, however, that u_2 and $\overline{u}_2$ remain unchanged, we can equate these two expressions and solve for c_1^*, t_1^*, and c_2^*. By eliminating c_1^* from the resulting equations, we find that the product of $t_1 c_1$ is an invariant quantity. Here we introduce

the bend parameter, k, as the ratio of t_1^*/t_1 and c_2/c_2^*. Returning this to the previous equations, we can solve for c_1^* in terms of the original system parameters and k. Next we write y_3 and $\bar{y}_3$ in terms of u_0, $\bar{u}_0$, y_1, $\bar{y}_1$, c_1, t_1, c_2, and t_2. Substituting changed values c_1^*, t_1^*, c_2^*, and t_2^* gives new values y_3^* and $\bar{y}_3^*$. By requiring that $y_3^* = y_3$ and $\bar{y}_3^* = \bar{y}_3$, and by using previously found expressions for c_1^*, t_1^*, and c_2^*, we can solve for t_2^* in terms of the original system parameters and k.

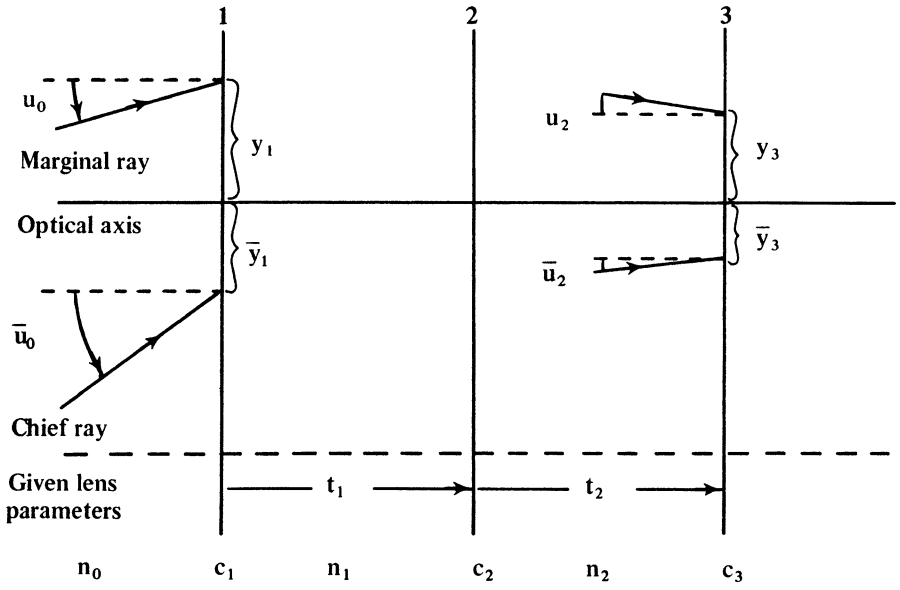

Figure 1. Bend derivation parameters. In the text, formulas are derived for modified values of the parameters c_1, t_1, c_2, and t_2, which will leave invariant the paraxial quantities shown here (above the dashed line). A family of solutions based on an arbitrary positive parameter, denoted by k, is obtained.

Details of the derivation follow. The paraxial refraction and transfer equations are (Hopkins and Hanau, 1962, p. 5-32)

$$n_j u_j = n_{j-1} u_{j-1} + y_j c_j (n_{j-1} - n_j) \tag{1}$$

and

$$y_j = y_{j-1} + (t_{j-1}/n_{j-1})(n_{j-1} u_{j-1}). \tag{2}$$

From Eqs. (1) and (2) we can write

$$n_2 u_2 = n_1 u_1 + y_2 c_2 (n_1 - n_2), \tag{3}$$

$$y_2 = y_1 + (t_1/n_1) n_1 u_1 \tag{4}$$

and

$$n_1 u_1 = n_0 u_0 + y_1 c_1 (n_0 - n_1). \tag{5}$$

Substituting Eq. (5) into Eq. (4) and then Eqs. (4) and (5) into Eq. (3), we obtain

$$n_2 u_2 = n_0 u_0 + y_1 c_1 (n_0 - n_1)$$

$$+ \{y_1 + (t_1/n_1)[n_0 u_0 + y_1 c_1 (n_0 - n_1)]\} c_2 (n_1 - n_2).$$

Expanding and collecting terms containing y_1 we have

$$n_2 u_2 - n_0 u_0 = y_1 [c_1 (n_0 - n_1) + c_2 (n_1 - n_2)$$

$$+ (t_1/n_1) c_1 (n_0 - n_1) c_2 (n_1 - n_2)]$$

$$+ n_0 u_0 (t_1/n_1) c_2 (n_1 - n_2). \tag{6}$$

The same equation can be written for the chief ray by substituting $\bar{u}_2$, $\bar{u}_0$, and $\bar{y}_1$ for u_2, u_0, and y_1, where

$$n_2 \bar{u}_2 - n_0 \bar{u}_0 = \bar{y}_1 [c_1 (n_0 - n_1) + c_2 (n_1 - n_2)$$

$$+ (t_1/n_1) c_1 (n_0 - n_1) c_2 (n_1 - n_2)]$$

$$+ n_0 \bar{u}_0 (t_1/n_1) c_2 (n_1 - n_2). \tag{7}$$

Then, assuming a system exists with slightly different values, we substitute c_1*, t_1*, c_2*, u_2*, and $\bar{u}_2$* for c_1, t_1, c_2, u_2, and $\bar{u}_2$, in Eqs. (6) and (7) where

$$n_2 u_2^* - n_0 u_0 = y_1 [c_1^* (n_0 - n_1) + c_2^* (n_1 - n_2)$$

$$+ (t_1^*/n_1) c_1^* (n_0 - n_1) c_2^* (n_1 - n_2)]$$

$$+ n_0 u_0 (t_1^*/n_1) c_2^* (n_1 - n_2), \tag{8}$$

and

$$n_2 \bar{u}_2^* - n_0 \bar{u}_0 = \bar{y}_1 [c_1^* (n_0 - n_1) + c_2^* (n_1 - n_2)$$

$$+ (t_1^*/n_1) c_1^* (n_0 - n_1) c_2^* (n_1 - n_2)]$$

$$+ n_0 \bar{u}_0 (t_1^*/n_1) c_2^* (n_1 - n_2). \tag{9}$$

Since we require that $u_2 = u_2^*$ and $\bar{u}_2 = \bar{u}_2^*$, the right sides of Eqs. (6) and (8) are equated and multiplied by $-\bar{y}_1$. Likewise, Eqs. (7) and (9) are equated and multiplied by y_1. These two equations are added. As a result, the terms in brackets in Eqs. (6), (7), (8), and (9) cancel, leaving

$$y_1 n_0 \bar{u}_0 (t_1/n_1) c_2 (n_1 - n_2) - \bar{y}_1 n_0 u_0 (t_1/n_1) c_2 (n_1 - n_2)$$

$$= y_1 n_0 \bar{u}_0 (t_1^*/n_1) c_2^* (n_1 - n_2) - \bar{y}_1 n_0 u_0 (t_1^*/n_1) c_2^* (n_1 - n_2).$$

Regrouping and canceling gives

$$(y_1 n_0 \bar{u}_0 - \bar{y}_1 n_0 u_0)t_1 c_2 = (y_1 n_0 \bar{u}_0 - \bar{y}_1 n_0 u_0)t_1 {}^* c_2 {}^*. \tag{10}$$

The first term in parentheses on both sides of the equation is easily recognized as the Lagrange invariant. Since the marginal and chief rays are separate and distinct, this quantity cannot equal zero. Therefore, Eq. (10) reduces to

$$t_1 c_2 = t_1 {}^* c_2 {}^*. \tag{11}$$

Now, to agree with the equations Sutton (1963) derived, the bend parameter k is introduced by defining

$$t_1 {}^* = k t_1 . \tag{12}$$

Substituting this into Eq. (11) gives

$$c_2 {}^* = c_2 / k. \tag{13}$$

Substituting Eqs. (11), (12), and (13) into Eq. (8) and equating this with Eq. (6), we can reduce the resulting equation to only the quantity in brackets on each side of the equation so that

$$c_1(n_0 - n_1) + c_2(n_1 - n_2) + (t_1/n_1)c_1(n_0 - n_1)c_2(n_1 - n_2)$$

$$= c_1 {}^*(n_0 - n_1) + (c_2/k)(n_1 - n_2) + (t_1/n_1)c_1 {}^*(n_0 - n_1)c_2(n_1 - n_2).$$

Transposing, factoring, and multiplying through by n_1 yields

$$(c_1 {}^* - c_1)(n_0 - n_1)[n_1 + t_1 c_2(n_1 - n_2)] = n_1 c_2(1 - 1/k)(n_1 - n_2).$$

We shall define $Q_1 = n_1 + t_1 c_2(n_1 - n_2)$. This is substituted into the preceding equation, which is then solved for $c_1 {}^*$, where

$$c_1 {}^* = c_1 + \frac{n_1 c_2(1 - 1/k)(n_1 - n_2)}{Q_1(n_0 - n_1)} . \tag{14}$$

Equations (12), (13), and (14) are the desired equations for a bend that will retain the slope angles u_2 and $\bar{u}_2$ as invariant. Next, we proceed to find the equation for $t_2 {}^*$ that will maintain y_3 and $\bar{y}_3$ constant. From Eq. (2) we can write

$$y_3 = y_2 + (t_2/n_2)n_2 u_2 , \tag{15}$$

and

$$y_2 = y_1 + (t_1/n_1)n_1 u_1 . \tag{16}$$

Substituting Eq. (5) into Eq. (16) we have

$$y_2 = y_1 + (t_1/n_1)[n_0 u_0 + y_1 c_1 (n_0 - n_1)]. \tag{17}$$

Substituting Eq. (17) and $n_2 u_2$ from Eq. (6) into Eq. (15), we obtain

$$\begin{aligned} y_3 = {} & y_1 + (t_1/n_1)[n_0 u_0 + y_1 c_1 (n_0 - n_1)] \\ & + (t_2/n_2)\{n_0 u_0 + y_1 [c_1 (n_0 - n_1) + c_2 (n_1 - n_2) \\ & + (t_1/n_1) c_1 (n_0 - n_1) c_2 (n_1 - n_2)] + n_0 u_0 (t_1/n_1) c_2 (n_1 - n_2)\}. \end{aligned}$$

Collecting terms containing y_1 and putting the remaining terms over the common denominator $n_1 n_2$ gives us

$$\begin{aligned} y_3 = {} & y_1 \{1 + (t_1/n_1) c_1 (n_0 - n_1) + (t_2/n_2)[c_1 (n_0 - n_1) \\ & + c_2 (n_1 - n_2) + (t_1/n_1) c_1 (n_0 - n_1) c_2 (n_1 - n_2)]\} \\ & + n_0 u_0 [n_2 t_1 + n_1 t_2 + t_1 t_2 c_2 (n_1 - n_2)]/n_1 n_2. \end{aligned} \tag{18}$$

Rewriting Eq. (18) for the chief ray by substituting $\bar{y}_3$, $\bar{y}_1$, and $\bar{u}_0$ for y_3, y_1, and u_0, we have

$$\begin{aligned} \bar{y}_3 = {} & \bar{y}_1 \{1 + (t_1/n_1) c_1 (n_0 - n_1) + (t_2/n_2)[c_1 (n_0 - n_1) \\ & + c_2 (n_1 - n_2) + (t_1/n_1) c_1 (n_0 - n_1) c_2 (n_1 - n_2)]\} \\ & + n_0 \bar{u}_0 [n_2 t_1 + n_1 t_2 + t_1 t_2 c_2 (n_1 - n_2)]/n_1 n_2. \end{aligned} \tag{19}$$

Substituting changed parameters c_1^*, t_1^*, c_2^*, t_2^*, y_3^*, and $\bar{y}_3^*$ for c_1, t_1, c_2, t_2, y_3, and $\bar{y}_3$ in Eqs. (18) and (19), we find

$$\begin{aligned} y_3^* = {} & y_1 \{1 + (t_1/n_1) c_1^* (n_0 - n_1) + (t_2^*/n_2)[c_1^* (n_0 - n_1) \\ & + c_2^* (n_1 - n_2) + (t_1^*/n_1) c_1^* (n_0 - n_1) c_2^* (n_1 - n_2)]\} \\ & + n_0 u_0 [n_2 t_1^* + n_1 t_2^* + t_1^* t_2^* c_2^* (n_1 - n_2)]/n_1 n_2 \end{aligned} \tag{20}$$

and

$$\begin{aligned} \bar{y}_3^* = {} & \bar{y}_1 \{1 + (t_1/n_1) c_1^* (n_0 - n_1) + (t_2^*/n_2)[c_1^* (n_0 - n_1) \\ & + c_2^* (n_1 - n_2) + (t_1^*/n_1) c_1^* (n_0 - n_1) c_2^* (n_1 - n_2)]\} \\ & + n_0 \bar{u}_0 [n_2 t_1^* + n_1 t_2^* + t_1^* t_2^* c_2^* (n_1 - n_2)]/n_1 n_2. \end{aligned} \tag{21}$$

Now we require that $y_3^* = y_3$ and $\bar{y}_3^* = \bar{y}_3$. The right sides of Eqs. (18) and (20) are equated and multiplied by $-\bar{y}_1$. Likewise, the right sides of Eqs. (19) and (21) are equated and multiplied by y_1. These equations are added. As a result, the terms in $\{\ \}$ in Eqs. (18), (19), (20), and (21) cancel leaving

$$y_1 n_0 \bar{u}_0 [n_2 t_1 + n_1 t_2 + t_2 t_1 c_2 (n_1 - n_2)]$$

$$- \bar{y}_1 n_0 u_0 [n_2 t_1 + n_1 t_2 + t_2 t_1 c_2 (n_1 - n_2)]$$

$$= y_1 n_0 \bar{u}_0 [n_2 t_1^* + n_1 t_2^* + t_2^* t_1^* c_2^* (n_1 - n_2)]$$

$$- \bar{y}_1 n_0 u_0 [n_2 t_1^* + n_1 t_2^* + t_2^* t_1^* c_2^* (n_1 - n_2)]. \qquad (22)$$

This can be factored and regrouped as

$$(y_1 n_0 \bar{u}_0 - \bar{y}_1 n_0 u_0)[n_2 t_1 + n_1 t_2 + t_2 t_1 c_2 (n_1 - n_2)]$$

$$= (y_1 n_0 \bar{u}_0 - \bar{y}_1 n_0 u_0)[n_2 t_1^* + n_1 t_2^* + t_2^* t_1^* c_2^* (n_1 - n_2)]. \qquad (23)$$

Again we see that the first factor on each side is the Lagrange invariant and therefore nonzero. Substituting Eqs. (11), (12), and (13) into Eq. (23) and reducing yields

$$n_2 t_1 + n_1 t_2 + t_1 t_2 c_2 (n_1 - n_2)$$

$$= n_2 k t_1 + n_1 t_2^* + t_1 t_2^* c_2 (n_1 - n_2).$$

By regrouping we find

$$t_2^* [n_1 + t_1 c_2 (n_1 - n_2)]$$

$$= t_2 [n_1 + t_1 c_2 (n_1 - n_2)] + t_1 n_2 (1 - k).$$

Substituting the previously defined Q_1 for the quantity in brackets and solving for t_2^* gives

$$t_2^* = t_2 + t_1 n_2 (1 - k)/Q_1. \qquad (24)$$

Equations (12), (13), (14), and (24) are the expressions that were desired for the four system quantities as functions of the bend parameter k. These equations are written in terms of the jth and j+1 surfaces and collected here:

$$c_j^* = c_j + \frac{n_j c_{j+1} (1 - 1/k)(n_j - n_{j+1})}{Q_1 (n_{j-1} - n_j)},$$

$$t_j^* = k t_j,$$

$$c_{j+1}^* = c_{j+1}/k,$$

$$t_{j+1}^* = t_{j+1} + t_j n_{j+1}(1 - k)/Q_1,$$

and

$$Q_1 = n_j + t_j c_{j+1}(n_j - n_{j+1}).$$

The preceding equations are considered to represent a "forward" bend at the jth and j+1 surfaces. A forward bend alters two curvatures and the thicknesses following each of these surfaces. The equations can be rewritten for a "backward" bend. This will alter two curvatures and the thickness preceding each of these surfaces. An optical system can be considered in the reverse sense; that is, rays are traced from image to object. Figure 2 illustrates such a reversed system. Note that the curvatures reverse signs but that the thicknesses and indices retain the previous values.

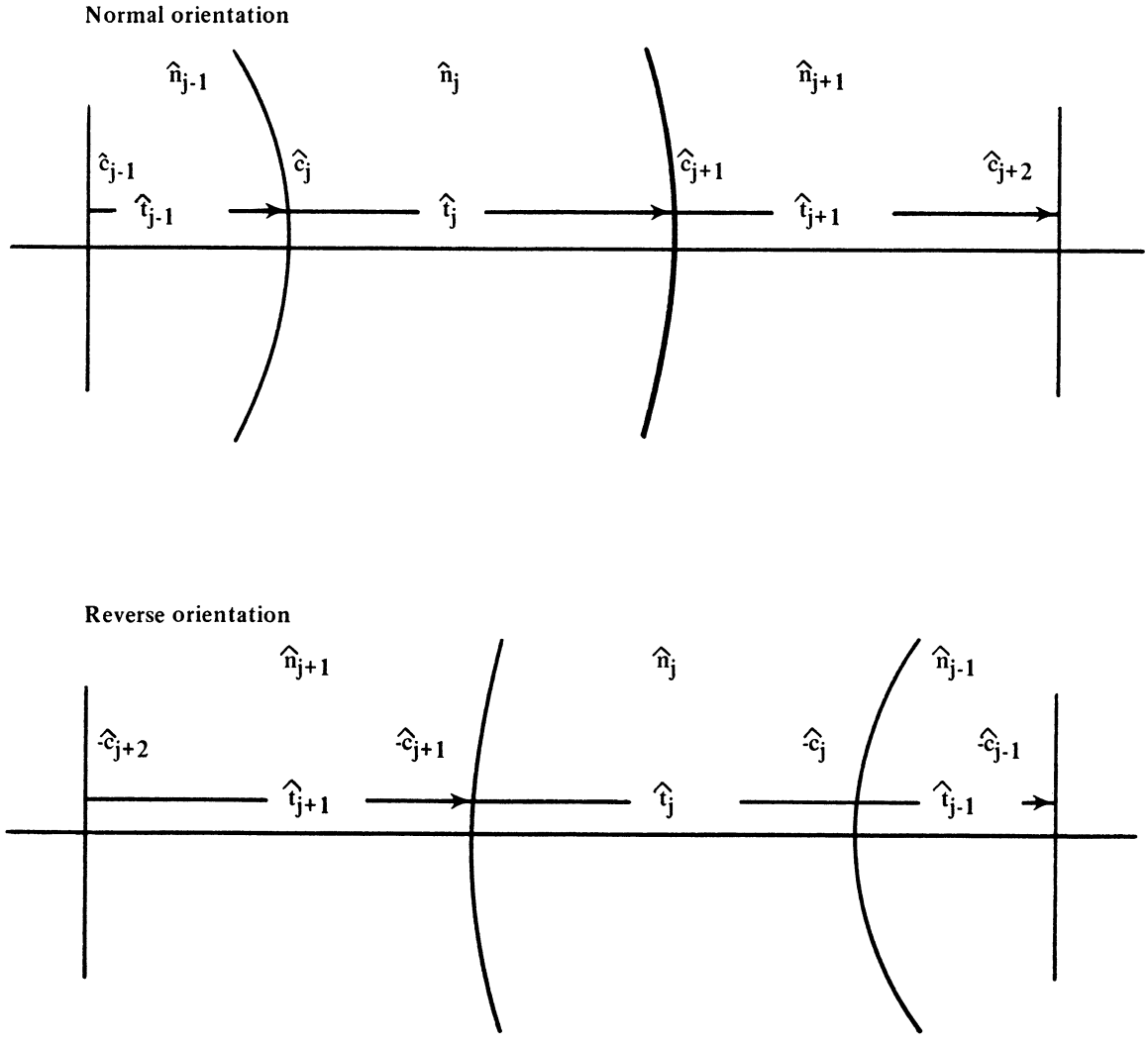

Figure 2. Backward bend diagram. In the text, bend equations are applied to a reversed optical system. The results are written in terms of a normal orientation, and the process is defined as a "backward" bend.

Applying the bend equation to this reversed system, we can see that c_j^* refers to the j+1 surface, t_j^* refers to $\hat{t}_j$, c_{j+1}^* refers to the jth surface, and t_{j+1}^* refers to $\hat{t}_{j-1}$. From this the following relations exist:

$$c_j = -\hat{c}_{j+1},$$

$$c_{j+1} = -\hat{c}_j,$$

$$t_j = \hat{t}_j,$$

$$t_{j+1} = \hat{t}_{j-1},$$

$$n_{j-1} = \hat{n}_{j+1},$$

$$n_j = \hat{n}_j,$$

and

$$n_{j+1} = \hat{n}_{j-1}.$$

Substituting these into the bend equations gives

$$Q_1 = \hat{n}_j + \hat{t}_j(-\hat{c}_j)(\hat{n}_j - \hat{n}_{j-1}),$$

$$c_j^* = -\hat{c}_{j+1} + \frac{\hat{n}_j(-\hat{c}_j)(1 - 1/k)(\hat{n}_j - \hat{n}_{j-1})}{Q_1(n_{j+1} - n_j)},$$

$$t_j^* = k\hat{t}_j,$$

$$c_{j+1}^* = -\hat{c}_j/k,$$

and

$$t_{j+1}^* = \hat{t}_{j-1} + \hat{t}_j\hat{n}_{j-1}(1 - k)/Q_1.$$

Returning to the normal direction, we can write

$$\hat{t}_{j-1}^* = t_{j+1}^*,$$

$$\hat{c}_j^* = -c_{j+1}^*,$$

$$\hat{t}_j^* = t_j^*,$$

and

$$\hat{c}_{j+1}^* = -c_j^*,$$

noting again that curvatures change sign. Combining these two sets of equations yields

$$\hat{t}_{j-1}^{*} = \hat{t}_{j-1} + \hat{t}_j \hat{n}_{j-1}(1 - k)/Q_1 ,$$

$$\hat{c}_j^{*} = \hat{c}_j / k,$$

$$\hat{t}_j^{*} = k\hat{t}_j,$$

and

$$\hat{c}_{j+1}^{*} = \hat{c}_{j+1} + \frac{\hat{n}_j \hat{c}_j (1 - 1/k)(\hat{n}_j - \hat{n}_{j-1})}{Q_1 (\hat{n}_{j+1} - \hat{n}_j)} ,$$

where

$$Q_1 = \hat{n}_j - \hat{t}_j \hat{c}_j (\hat{n}_j - \hat{n}_{j-1}).$$

These equations will henceforth refer to a "backward" bend at the jth and j+1 surfaces.

CHAPTER 2

PHYSICAL CHANGES TO LENS

In this chapter we discuss the physical effect on a particular lens. For the purpose of this study we have arbitrarily chosen a 100-mm, F/3.5 triplet (Fig. 3). In the following chapters the effects of the application of the preceding formulas to this lens will be discussed from the standpoint of the effects upon real rays traced through the lens and upon aberration coefficients.

Sutton (1963) discussed the singularity that occurs when Q_1 in the equations for c_j^* and t_{j+1}^* for a forward bend goes to zero. This quantity is an invariant function of the original lens and does not change during a bend operation. Evaluating Q_1 for extreme values of its parameters will show that Q_1 can equal zero only in relatively widely spaced systems such as a relay. Recalling that Q_1 is defined as

$$Q_1 = n_j + t_j c_{j+1}(n_j - n_{j+1}),$$

then Q_1 can equal zero only when

$$t_j c_{j+1}(n_j - n_{j+1}) = -n_j.$$

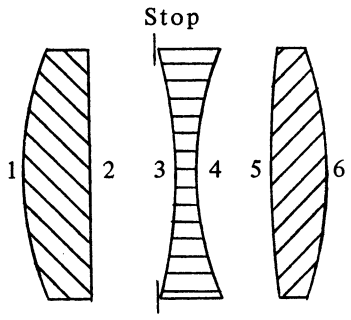

LENS SPECIFICATION

Surface	Radius of curvature (mm)	Thickness (mm)*	Refractive index*	Abbe number*
1	37.1	7.4	1.59015	61.0
2	∞	8.1	1.0	
Stop		1.8	1.0	
3	-55.0	2.6	1.62377	35.7
4	36.7	8.7	1.0	
5	127.0	6.4	1.62176	53.0
6	-43.2	81.5	1.0	
Image plane				

*Of medium following the surface

Figure 3. Triplet. This is the original 100-mm, F/3.5 triplet (Merte, 1950) used for the investigation of generalized bending.

The normal extreme for $n_j - n_{j+1}$ is about -0.8, and the minimum value of n_j is obviously 1.0. Substituting $1/r_{j+1}$ for c_{j+1} and these values into the last equation yields

$$t_j = 1.25 r_{j+1}.$$

This means that the thickness preceding a surface would have to be greater than the radius of curvature of the surface. In this triplet the greatest thickness is 9.9 mm, while the shortest radius is 36.7 mm. In discussing this singularity, it will suffice to note that Q_1 will always be positive. Later we will consider the importance of the magnitude of Q_1.

The next point of interest becomes apparent from looking at the equation for c_j^*:

$$c_j^* = c_j + \frac{n_j c_{j+1}(1 - 1/k)(n_j - n_{j+1})}{Q_1(n_{j-1} - n_j)}.$$

The change in the curvature of the first of a pair of surfaces being bent is directly dependent upon the original curvature of the second. If the second surface is plane, $c_{j+1} = 0$, there will be no change to the curvature of the first surface. Since the first element of the triplet being considered here is convex-plano, this situation will occur in this investigation. It does not present any apparent problems, but it will be considered further in the discussion of the nodes in the next chapter. Note, however, that a backward bend at the same two surfaces will change both curvatures.

Before proceeding, note that when k = 1.0, the bend equations degenerate to the original value of the parameters. Therefore, k = 1.0 represents the original lens with no change. Depending on the value of the bend parameter k, a change of sign of the lens parameters c_j, t_j, c_{j+1}, and t_{j+1}, may occur. In the case of curvatures, this is entirely acceptable and may be desired. However, a change in the sign of the thickness following a refractive or reflective surface is a meaningless result. Such a change must be either prevented or controlled.

The first and easiest case to dispose of is t_j. Since $t_j^* = kt_j$, t_j will change signs only if k has a negative value. Thus we must restrict k to positive values. We look next at c_{j+1} because it is closely related to t_j. This restriction on k will also prevent a change of sign of c_{j+1}. To cause the curvature of a surface to change signs, it must enter the bend equations as c_j. From the equation for c_j^*, we can see that the magnitude of k and the sign of c_{j+1} will control the sign of the second term in the equation. (Again, it is assumed that Q_1 is positive.) The sign of c_j will change if the second term is of greater magnitude than c_j and of opposite sign. As stated earlier, this change of sign may be desirable so it need not be prevented or controlled. Thus, by restricting k to positive values, it is certain that c_j^*, t_j^*, and c_{j+1}^* will all be valid quantities until their magnitudes are carried to extremes.

The remaining "bent" parameter t_{j+1}^* is not as easily controlled as the previous three. Like t_j^*, it must retain its original sign, but like c_j^*, many parameters control it. The equation for t_{j+1}^* yields

$$t_{j+1}^* = t_{j+1} + [n_{j+1} t_j (1 - k)]/Q_1 .$$

We note that t_{j+1}, n_{j+1}, t_j, and Q_1 are all positive quantities. If k is greater than one, then the second term becomes negative. If the magnitude of the second term is greater than t_{j+1}, then it will cause t_{j+1}^* to become negative. Again, this is a physically meaningless value. By restricting the maximum value of k to one, we could prevent this occurrence, but that would be overly restrictive for the bending available to the other three system parameters. For this reason, rather than suggest a restriction on the value of k, we will return to the equation for t_{j+1}^* to see when it is likely to occur. Substituting $1/r_{j+1}$ for c_{j+1}, we can write the equation for Q_1 as

$$Q_1 = n_j + (t_j/r_{j+1})(n_j - n_{j+1}).$$

We can show that the second term is generally quite small, therefore $Q_1 \approx n_j$. In our triplet the maximum value of the ratio t_j/r_{j+1} occurs for a backward bend at surfaces five and six. In this case, $t_j = 8.7$ and $r_{j+1} = 36.7$, which yields a ratio of 0.24, while the value for $(n_j - n_{j+1})$ is 0.62377. These values make the magnitude of the second term in the equation 0.15. This is much less than any possible n_j. Therefore, for rough

approximation the formula for t_{j+1}^* could be written

$$t_{j+1}^* \approx t_{j+1} + (n_{j+1}/n_j)t_j(1 - k).$$

Obviously there is always a value for k that will cause the second term to be greater than t_{j+1}. This value will depend mainly on the ratio of n_{j+1}/n_j and t_j/t_{j+1}. Generally, the ratio n_{j+1}/n_j will be less than one when the two surfaces being bent define a glass element and will be greater than one when the two surfaces bound an air space. The maximum value of k used in any investigation in connection with this report was k = 2.0. A negative thickness resulted each time both n_{j+1}/n_j and t_j/t_{j+1} were greater than one for this value of k. At no other time did it occur. In other words, a thick air space followed by a thinner glass element always resulted in a meaningless bend at k = 2.0. As the ratio t_j/t_{j+1} increased greater than one, a negative thickness occurred for smaller values of k.

While I have stated that a negative thickness is a meaningless situation, this should be qualified. An intermediate negative thickness would be acceptable if a subsequent bend at another pair of surfaces were used to correct the sign (see Figs. 4 through 6). Such a procedure might be useful in some situations. Nevertheless, one must be alert to the occurrence of a negative thickness; the previous discussion shows when this is likely.

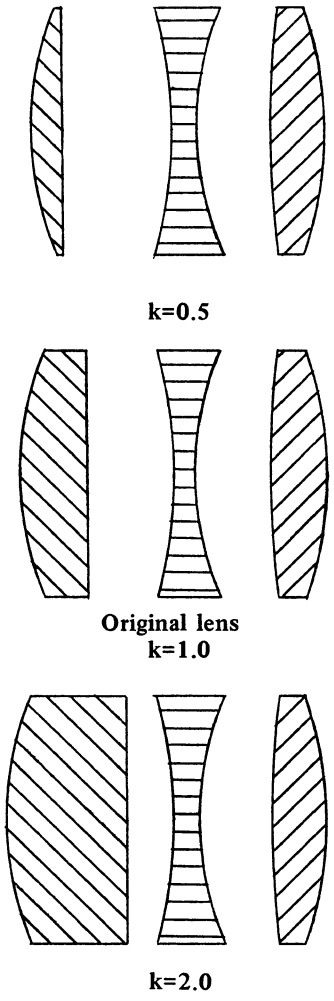

Figure 4. Change to triplet, forward bend at surfaces 1 and 2. Since the second surface is plane, no curvatures change. Thicknesses on both sides of the plane surface do change.

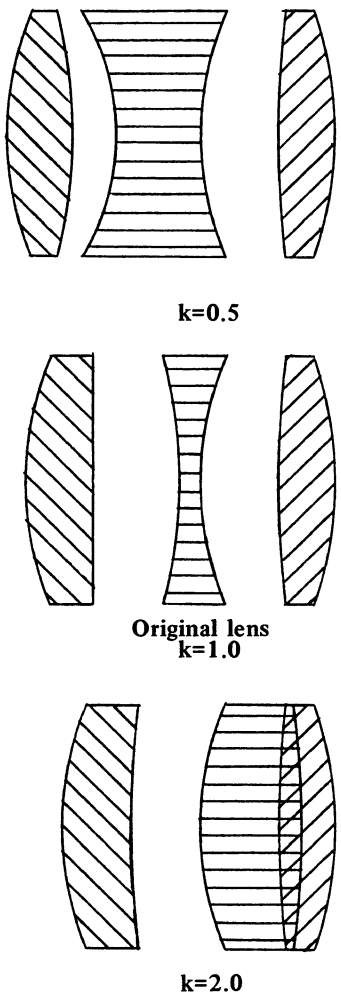

Figure 5. Change to triplet, forward bend at surfaces 2 and 3. When a plane surface is the first of a pair of surfaces being bent, it assumes both positive and negative curvatures depending on k. The thickness following the third surface has become negative for k = 2.0.

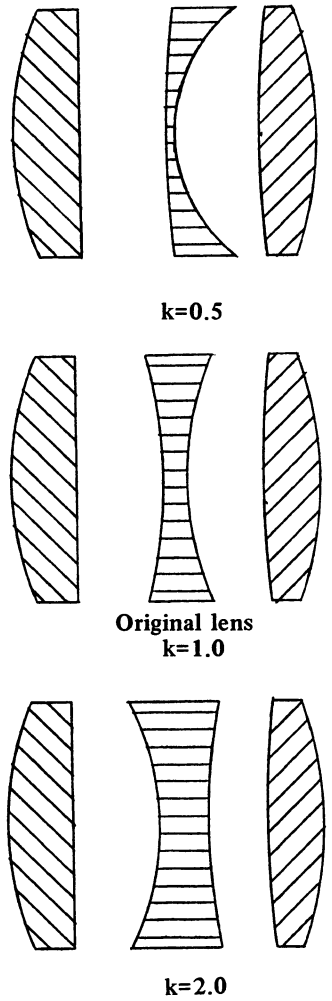

Figure 6. Change to triplet, forward bend at surfaces 3 and 4. This represents a smooth, normal bend with the first surface of the pair being bent, assuming both positive and negative curvatures.

CHAPTER 3

THE EFFECTS OF BENDING ON REAL RAYS

Most of the information presented in this report resulted from data generated using the General Electric Time Sharing Service MARK I and MARK II from the terminal at the Optical Sciences Center. All of the programs were written in BASIC language except one, ABERAT, which was written in FORTRAN.

Initially, not having well-defined goals, I attempted to learn something about generalized bending equations. The first program, BREAK, was written to perform a paraxial ray trace for marginal and chief rays for a given lens. From these ray traces, error coefficients were calculated using the formulations given by Feder (1951, pp. 632 and 633). The forward bend equations were then applied to the lens for five values of the bend parameter.

Each pair of surfaces of the lens was bent starting at the front and proceeding through the lens. The new image error coefficients were calculated and printed out for each surface as it was bent and also for each value of the bend parameter. This immediately generated an overwhelming amount of data. An attempt to check the calculations by comparing them with a run on the University of Arizona CDC 6400 computer using Scientific Calculations Inc. ACCOS-GOALS program pointed out the fact that image error coefficients were being calculated differently. This approach was abandoned temporarily in favor of looking at the effect of bending upon a real ray traced through the lens.

At this point, I decided to switch to the notation and formulation of Hopkins and Hanau (1962) given in *MIL-HDBK-141* for all future calculations. The portion of the program BREAK that actually performed the bending calculations did not involve the changed notation. It was used to provide a data file, BENT. This file contained lens parameters for five values of k and for all possible forward and backward bends.

A new program, REALRA, was written that traced real rays through an optical system. The program was set up to trace 33 rays for each particular bend situation. These rays included meridional and skew fans for three field positions and an axial fan. For each field position the chief ray through the original lens was traced first, and its height in the image plane was subtracted from the Y height of all the other rays' Y heights in the image plane. The chief ray height and the difference for the other rays were printed out as well as the X coordinate in the image plane for the skew rays. Basically, the ray tracing and the data plotting were done following the technique set forth by Hopkins (1962, pp. 9-5 and 9-6) in *MIL-HDBK-141* (see Figs. 7 through 16).

It is difficult to make a general statement about the effect of bending on these plots. Bends at some surfaces produce a smooth fanning out of the curves (Figs. 7, 9, 13, and 14). At other surfaces, the bends weave the curves in a complex manner (Figs. 8 and 15). However, in no case did the bending generally displace the curves relative to each other. In one zone of the aperture the curves would separate, but at some other zone the curves invariably remained in close relative proximity. At their closest point the curves for a full range of bends did not differ by more than 0.4 mm. This is less than 1% of the format size.

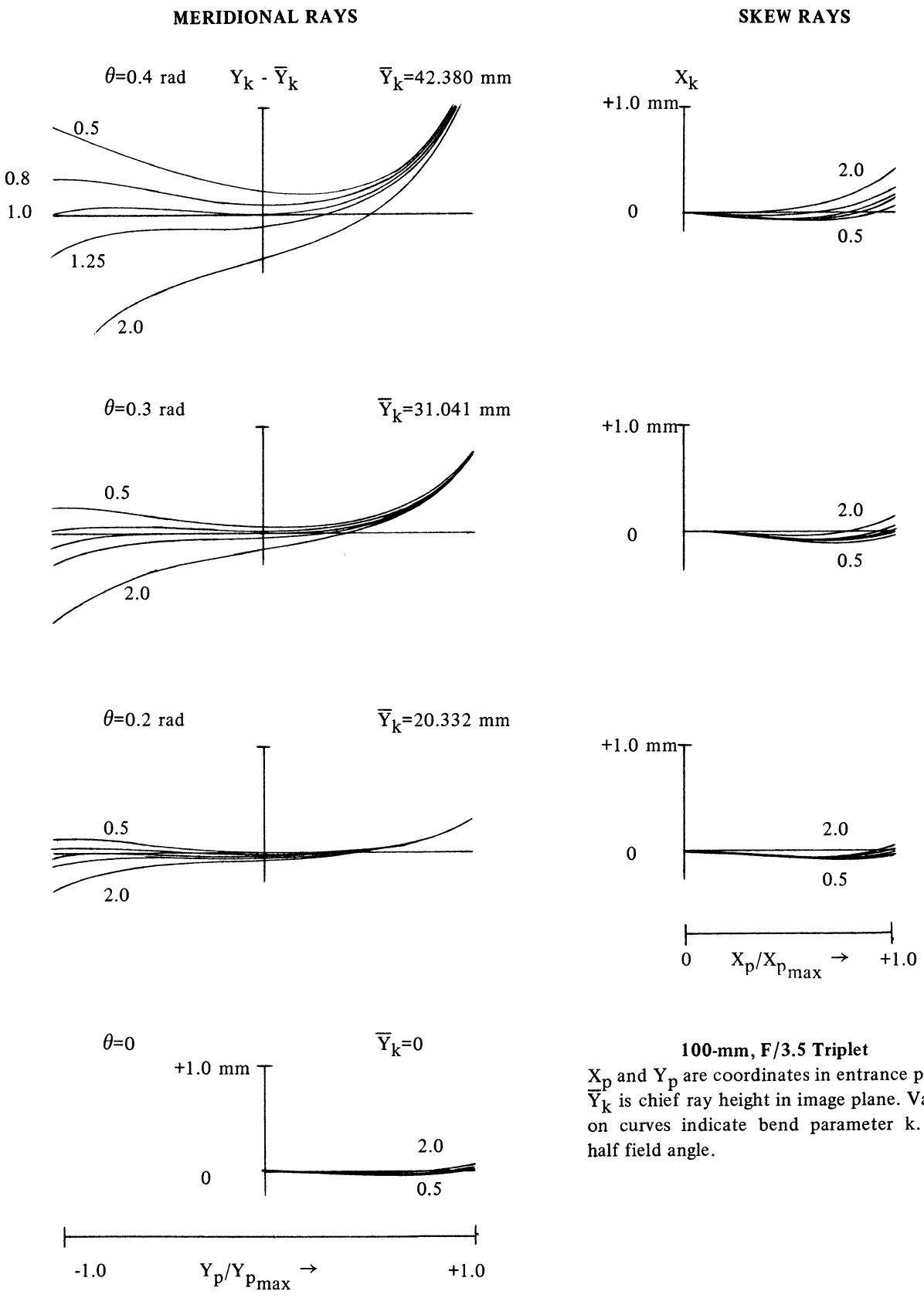

100-mm, F/3.5 Triplet

X_p and Y_p are coordinates in entrance pupil. $\bar{Y}_k$ is chief ray height in image plane. Values on curves indicate bend parameter k. θ is half field angle.

Figure 7. Ray fan plot—forward bend at surfaces 1 and 2.

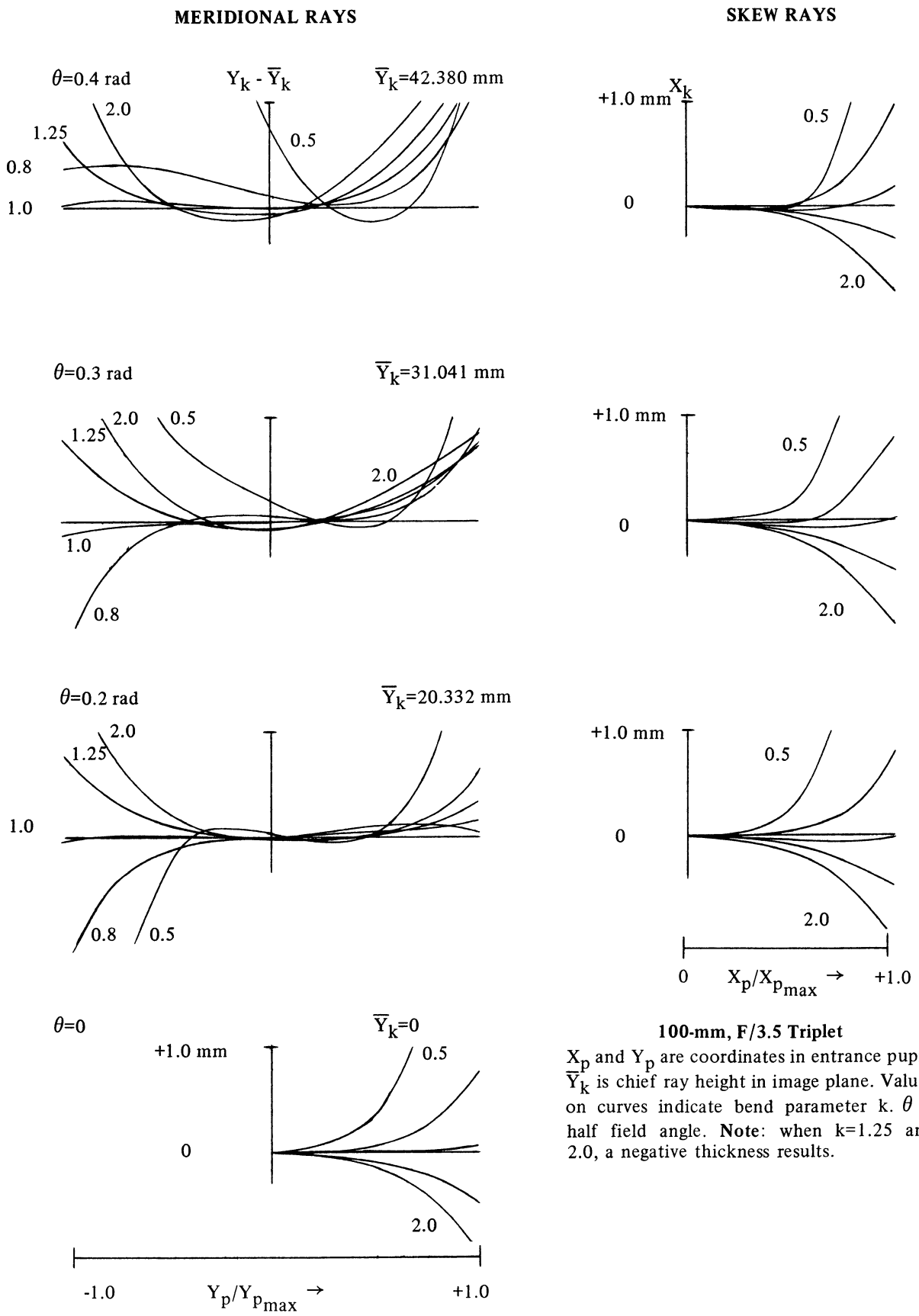

100-mm, F/3.5 Triplet

X_p and Y_p are coordinates in entrance pupil. $\bar{Y}_k$ is chief ray height in image plane. Values on curves indicate bend parameter k. θ is half field angle. **Note**: when k=1.25 and 2.0, a negative thickness results.

Figure 8. Ray fan plot—forward bend at surfaces 2 and 3.

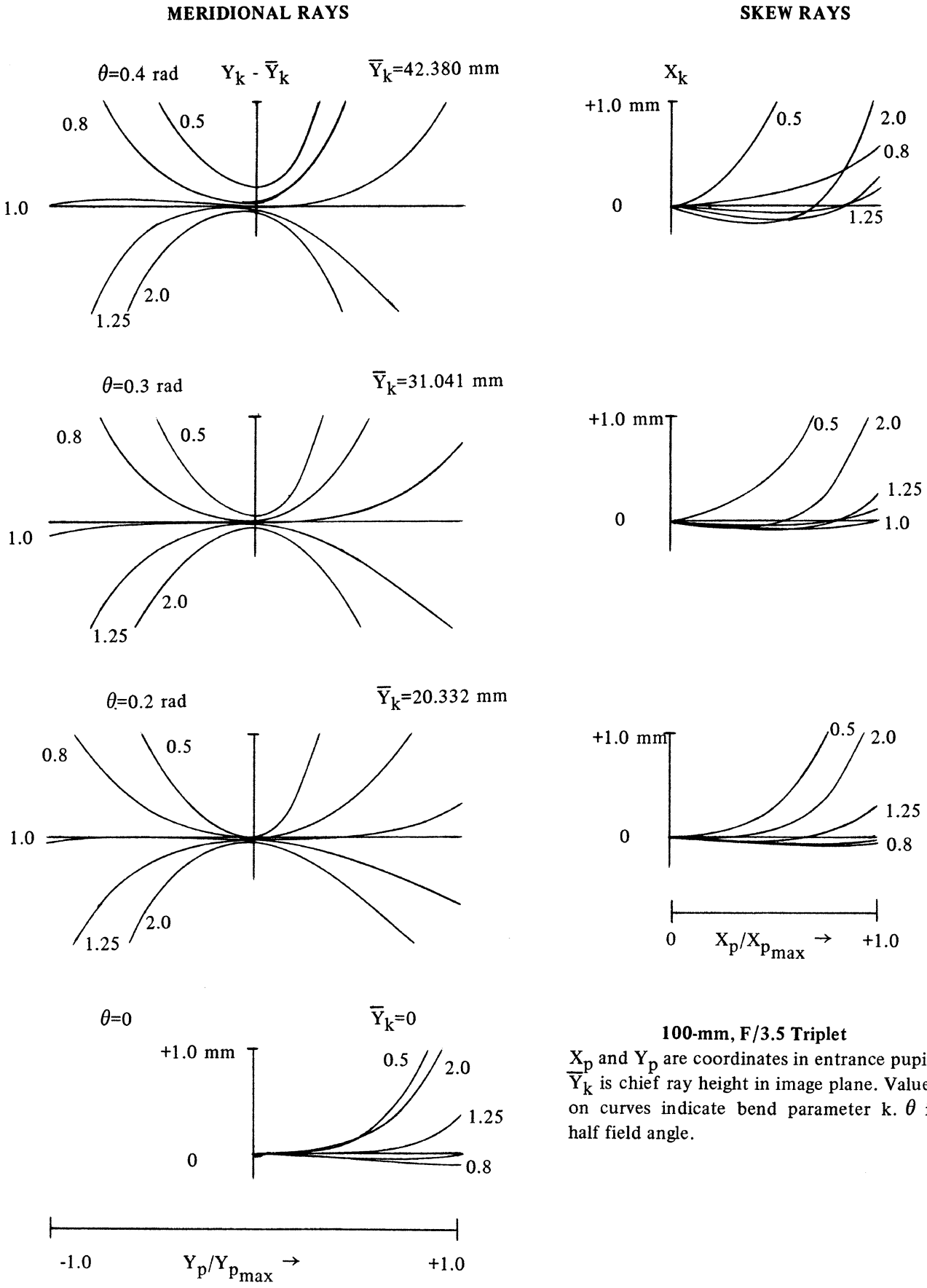

100-mm, F/3.5 Triplet

X_p and Y_p are coordinates in entrance pupil. $\overline{Y}_k$ is chief ray height in image plane. Values on curves indicate bend parameter k. θ is half field angle.

Figure 9. Ray fan plot—forward bend at surfaces 3 and 4.

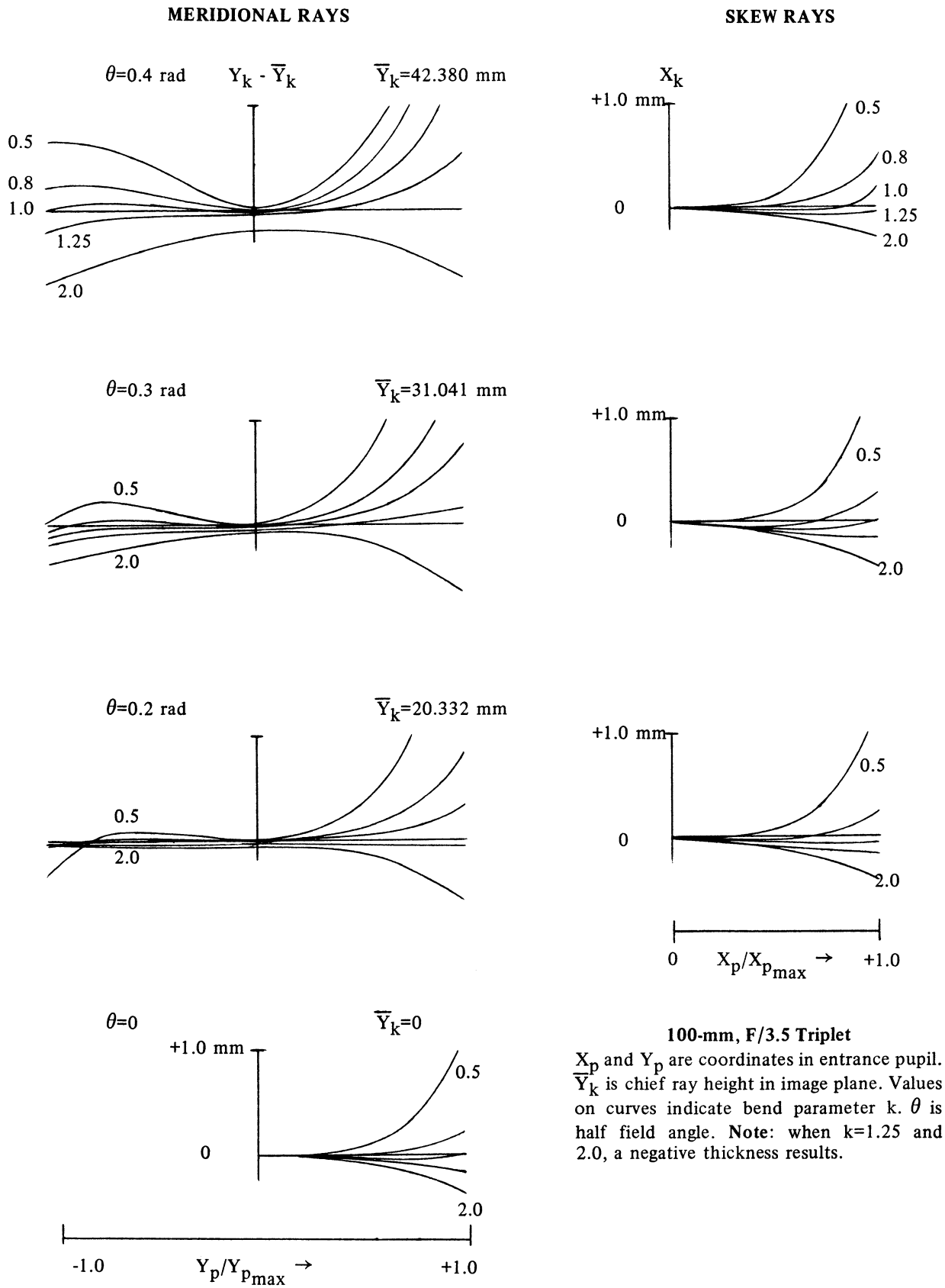

100-mm, F/3.5 Triplet

X_p and Y_p are coordinates in entrance pupil. $\overline{Y}_k$ is chief ray height in image plane. Values on curves indicate bend parameter k. θ is half field angle. **Note**: when k=1.25 and 2.0, a negative thickness results.

Figure 10. Ray fan plot—forward bend at surfaces 4 and 5.

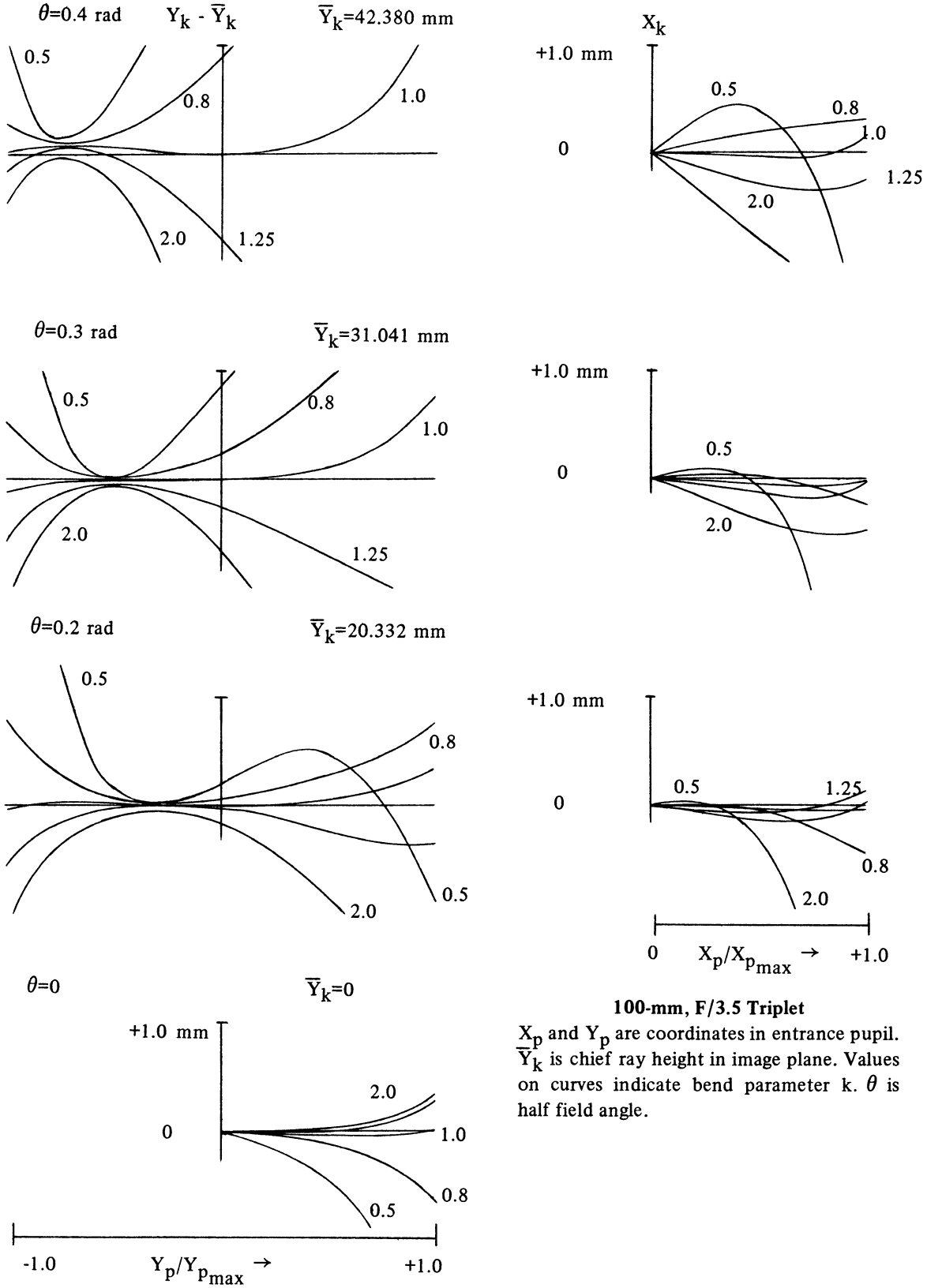

100-mm, F/3.5 Triplet

X_p and Y_p are coordinates in entrance pupil. $\bar{Y}_k$ is chief ray height in image plane. Values on curves indicate bend parameter k. θ is half field angle.

Figure 11. Ray fan plot–forward bend at surfaces 5 and 6.

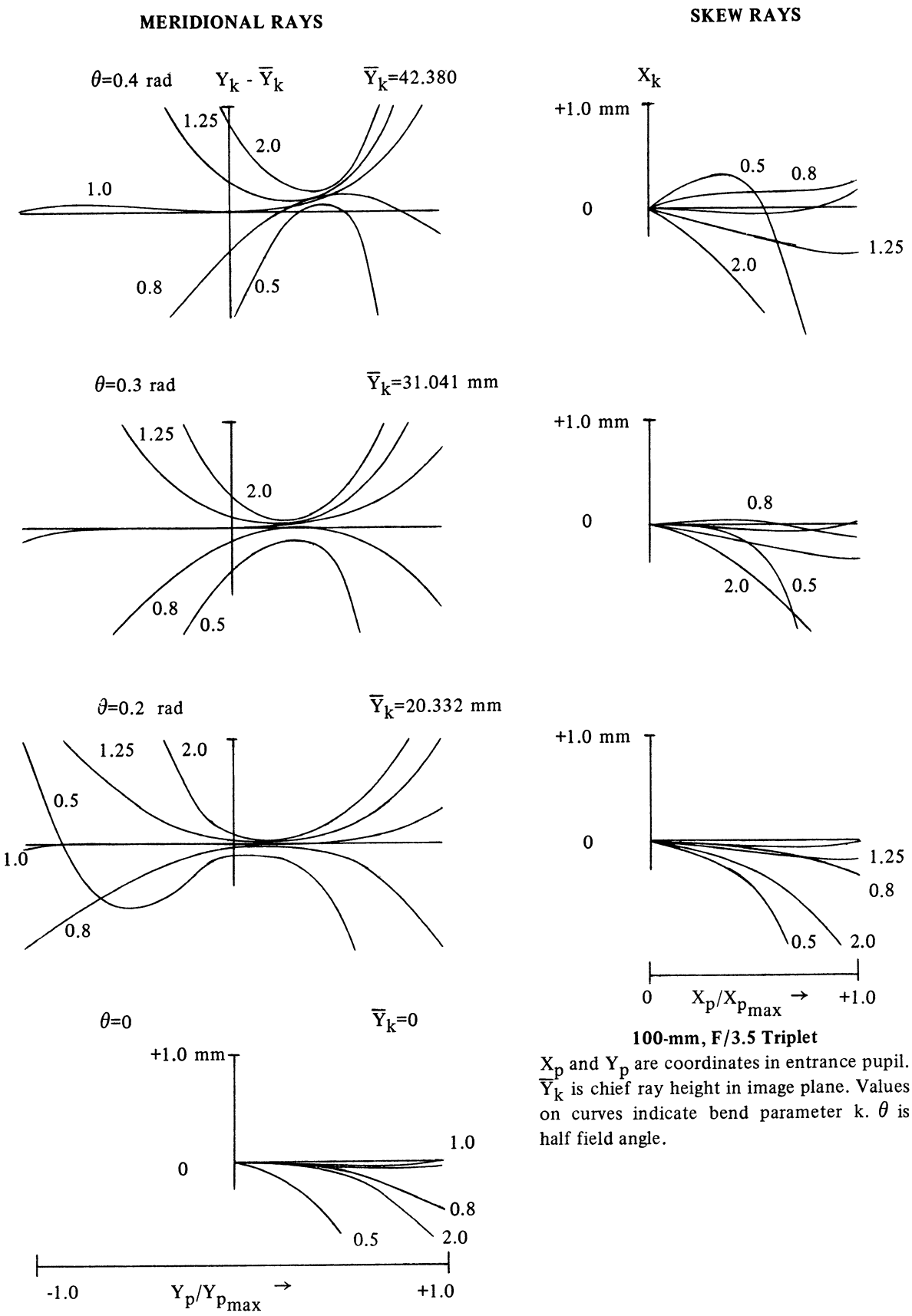

100-mm, F/3.5 Triplet

X_p and Y_p are coordinates in entrance pupil. $\bar{Y}_k$ is chief ray height in image plane. Values on curves indicate bend parameter k. θ is half field angle.

Figure 12. Ray fan plot—backward bend at surfaces 1 and 2.

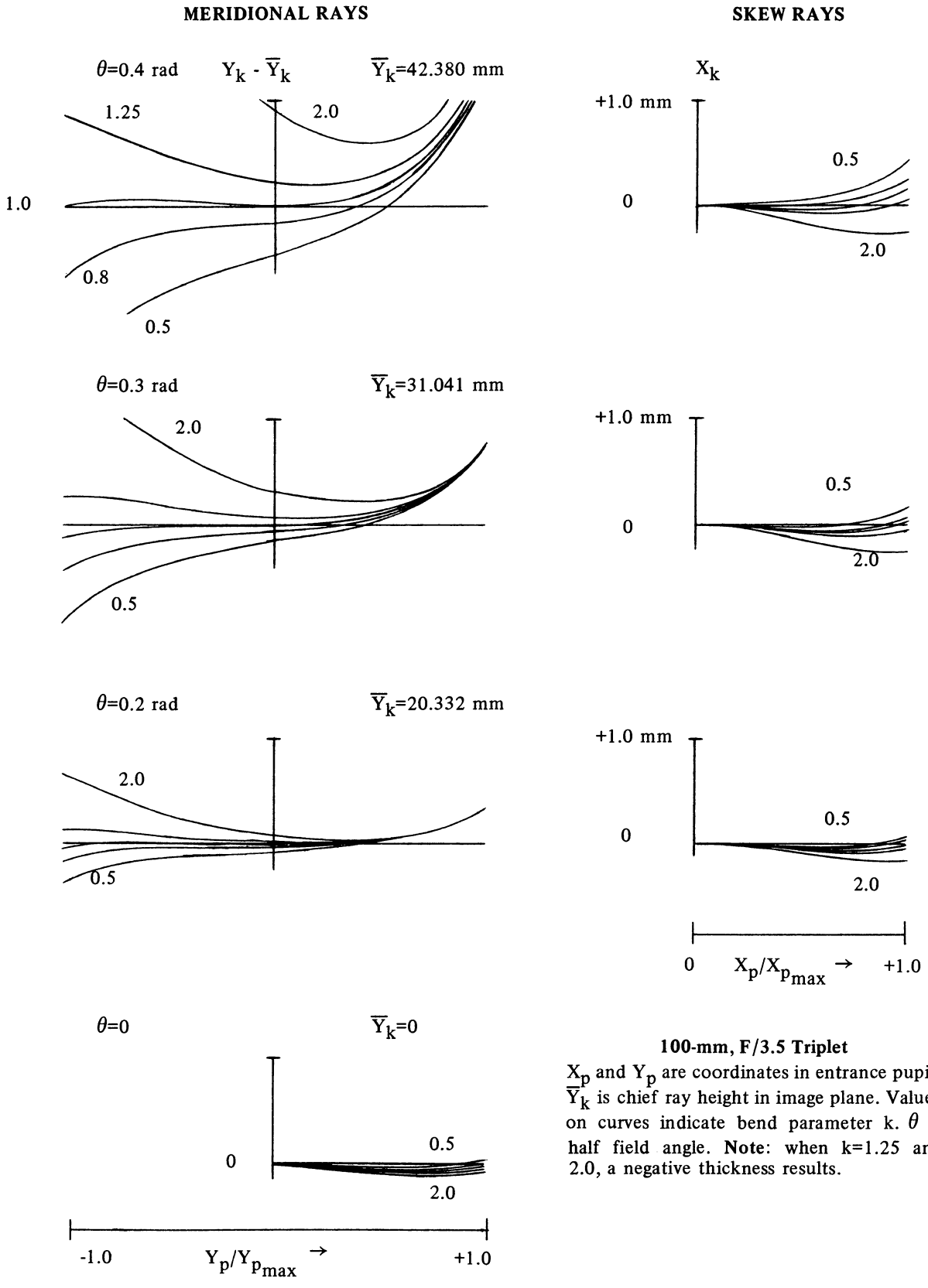

100-mm, F/3.5 Triplet

X_p and Y_p are coordinates in entrance pupil. $\bar{Y}_k$ is chief ray height in image plane. Values on curves indicate bend parameter k. θ is half field angle. **Note**: when k=1.25 and 2.0, a negative thickness results.

Figure 13. Ray fan plot—backward bend at surfaces 2 and 3.

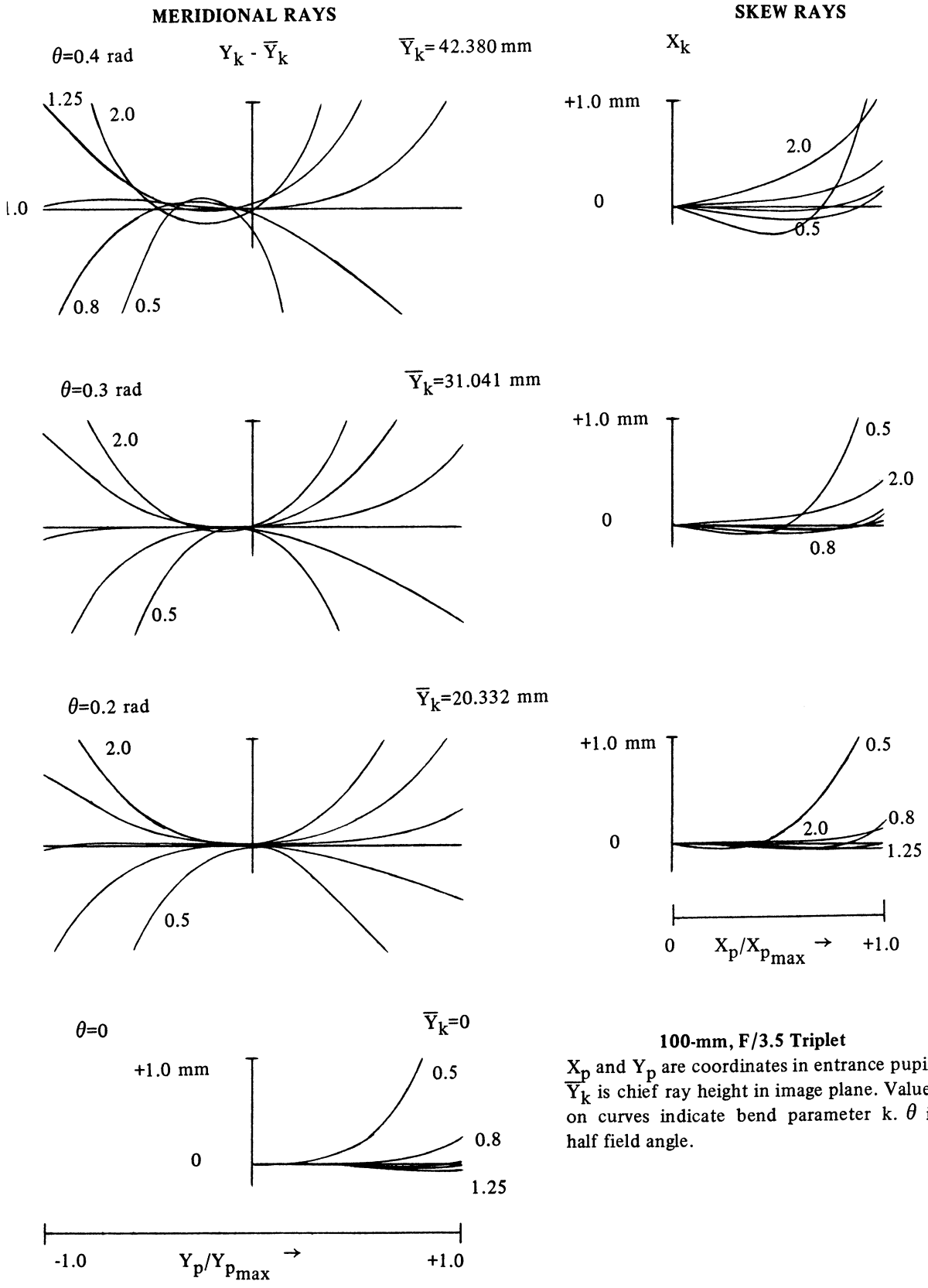

100-mm, F/3.5 Triplet

X_p and Y_p are coordinates in entrance pupil. $\overline{Y}_k$ is chief ray height in image plane. Values on curves indicate bend parameter k. θ is half field angle.

Figure 14. Ray fan plot—backward bend at surfaces 3 and 4.

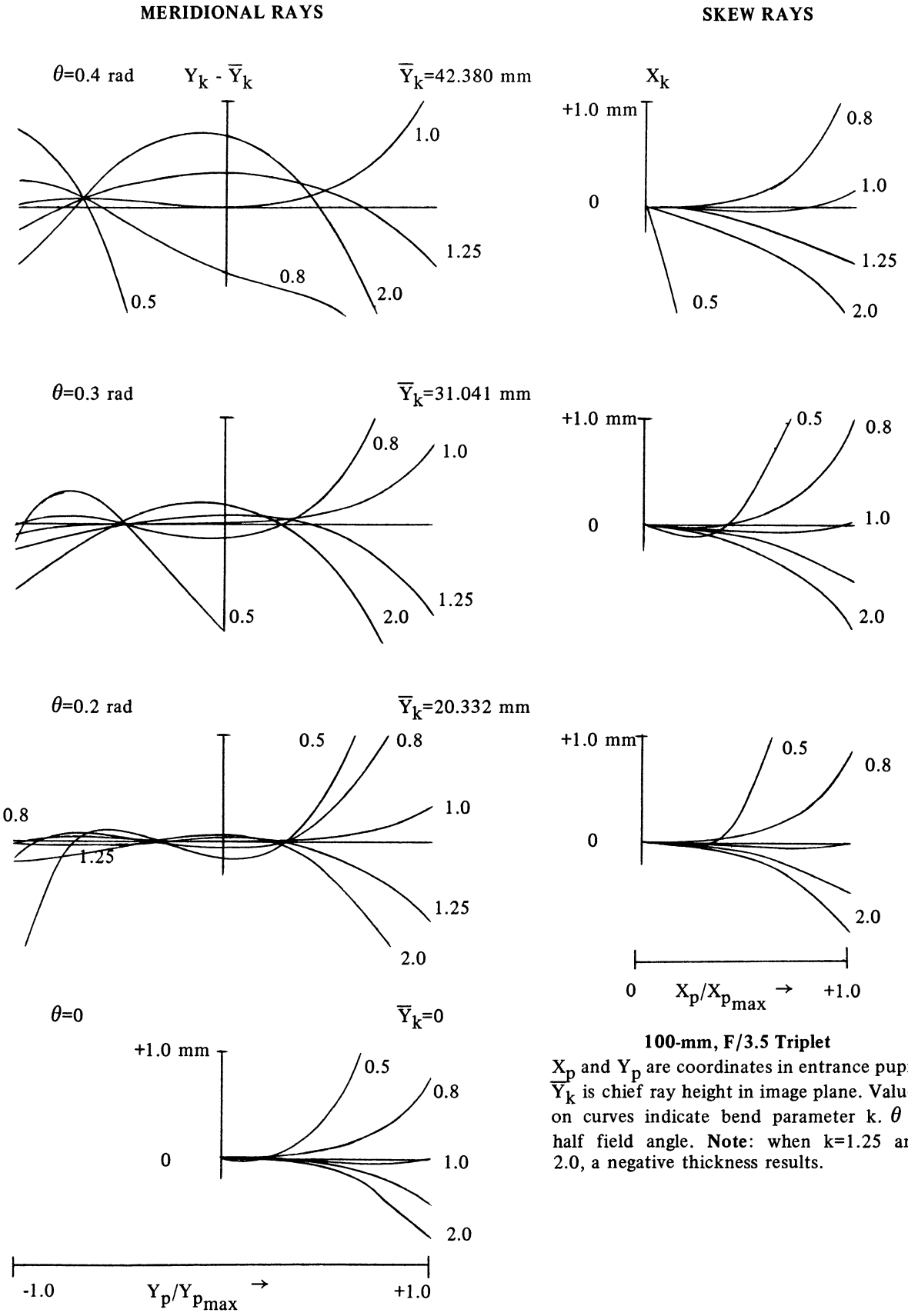

100-mm, F/3.5 Triplet

X_p and Y_p are coordinates in entrance pupil. $\overline{Y}_k$ is chief ray height in image plane. Values on curves indicate bend parameter k. θ is half field angle. **Note**: when k=1.25 and 2.0, a negative thickness results.

Figure 15. Ray fan plot—backward bend at surfaces 4 and 5.

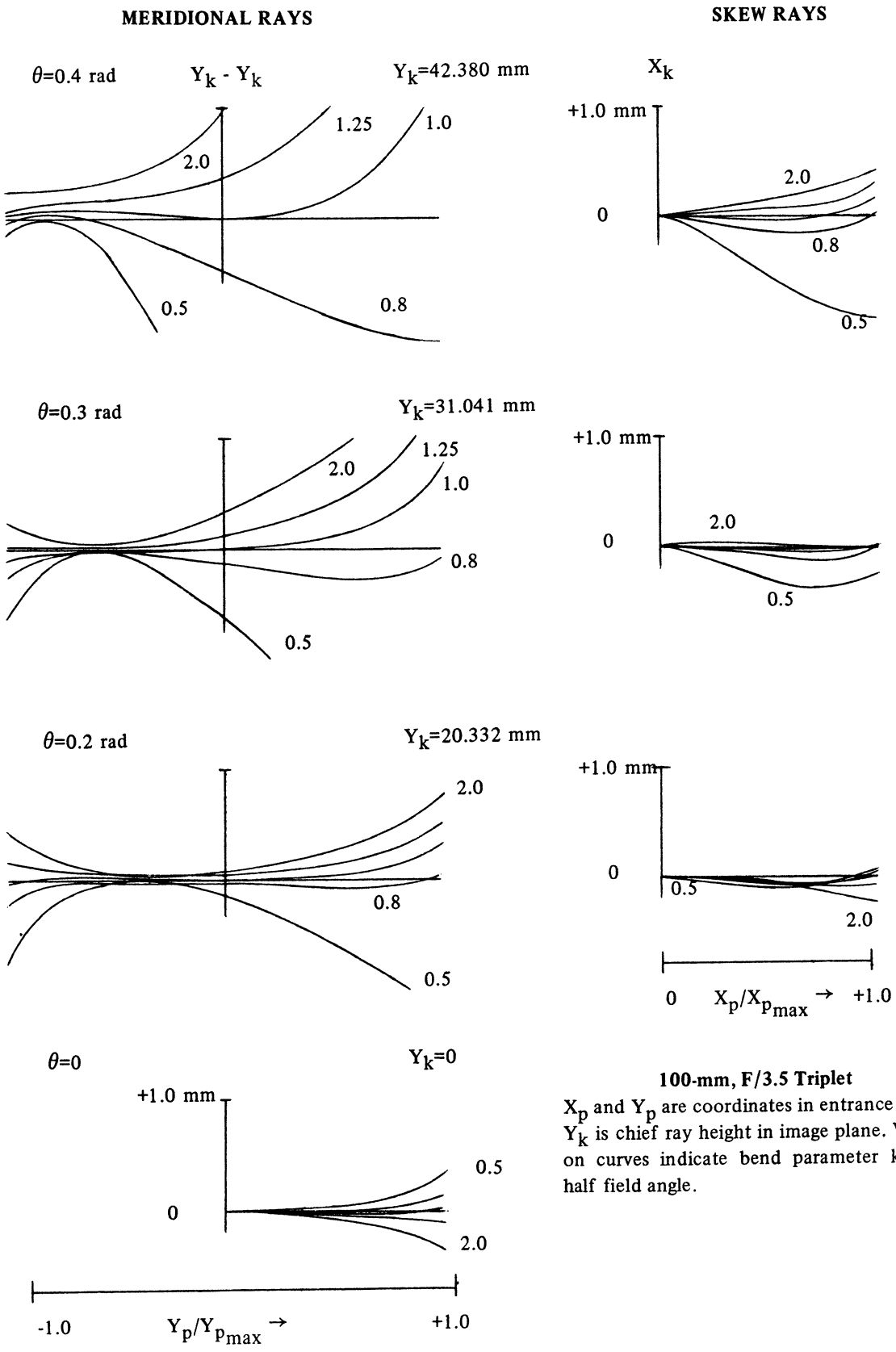

100-mm, F/3.5 Triplet

X_p and Y_p are coordinates in entrance pupil. Y_k is chief ray height in image plane. Values on curves indicate bend parameter k. θ is half field angle.

Figure 16. Ray fan plot—backward bend at surfaces 5 and 6.

At some surfaces the curves appeared to form a very pronounced node resembling a vibrating string node. This node identifies a special point in the entrance pupil. The position in the image plane of a real meridional ray through this point in the entrance pupil is unchanged by bending. The most striking example of this occurred with a backward bend at the pair of surfaces that comprise the second air space in the lens (Fig. 15). As pointed out in the previous chapter, a bend at an air space unfortunately caused a negative thickness for a bend parameter only slightly greater than one. Nevertheless, for $k \approx 1$ a bend at this location does offer a smooth change in aberrations. In this case there were two very pronounced nodes. There was usually only one node associated with each possible bend. Generally, the location of the node progressed from one side of the pupil to the other as the location of the bend operation was moved from the left end of the lens to the right.

The node associated with the forward bend at the first element of the lens was studied in some detail (Figs. 7 and 14). A ray with a half-field angle of 0.2 radian through the top of the entrance pupil was changed by less than 10^{-6} mm in the image plane as bending occurred. Then, when backward bends were performed on the first air space of the lens, the same rays went through with exactly the same intercept in the image plane. Finally it was realized that both of these bends occurred at the plane surface of the lens with the plane surface entering the bend equation so that no curvatures were changed, as was pointed out in Chapter 2.

The particular ray that was unchanged in the image plane by the bending was a ray that was rendered parallel to the optical axis after refraction at the first surface and thus was normal to the plane surface. Since only thickness changes occurred on each side of the plane surface, this ray obviously would be unchanged. This does not necessarily remove interest from this node. The plot of rays as bending occurred at this pair of surfaces did represent the smoothest fan of all the plots. Plane surfaces in optical systems may generally exhibit this smooth family of plots. If so, they might be of great usefulness as in the following application: If a pair of surfaces can be found that produces a node about which intercept plots are fanned out smoothly, perhaps a prior bend at some other surfaces could be used to locate this node on the axis of the intercept plot. This of course means that the stable ray would intercept the image plane at the same point as the chief ray. Then, bends at the location giving the fan of curves might provide considerable control over the intercept plots. For example, assume a forward bend at surfaces three and four (Fig. 9) with $k = 1.1$. This would move the node associated with a forward bend at surfaces one and two (Fig. 7) down to the axis. Then a plot of a new fan of rays for bends at surfaces one and two might show a further bend that would provide considerable correction to the lens.

CHAPTER 4

THE EFFECTS OF BENDING ON SEIDEL CONTRIBUTIONS

A new program, BREAK2, was written to calculate the five Seidel contributions plus the contribution to primary axial and lateral color (Hopkins, 1962, pp. 9-11). This program was written so that for each bend situation the new sum of the contributions of all surfaces and the change in each sum from the original lens would be printed out for each Seidel error and color coefficient. This still represented an overwhelming amount of data. I decided to try to describe the change in each coefficient as a polynomial function of k.

The Seidel contributions are third-order quantities based on first-order ray information. If a bend is made at the first and second surfaces of a lens, the first-order ray data at the third and subsequent surfaces will be unchanged. Therefore, the Seidel contribution of these latter surfaces also is unchanged. Likewise, a bend at the third and fourth surfaces changes the Seidel contributions of these surfaces alone. Thus, an optical system could be separated into independent pairs of adjacent surfaces yielding a maximum number of independent bends equal to one half the number of effective surfaces. The term effective surfaces is used to point out such things as the difference between a cemented and an air-spaced doublet. The former has only three effective surfaces, and thus only one independent bend is possible, while an air-spaced doublet has four effective surfaces, and two independent bends are possible.

The triplet presented in Chapter 2 has six independent surfaces; thus there are three possible independent bends. As a straightforward but rather arbitrary decision, the triplet was set up for three independent forward bends at the first and second, third and fourth, and fifth and sixth surfaces. It should be noted that the choice could have been three backward bends or a backward bend at the first and second surfaces with a forward bend at the fifth and sixth surfaces and either a forward or a backward bend at the two middle surfaces. Since there were only three simultaneous independent bends possible, I decided to restrict the rest of this investigation to reduction of the coefficients for spherical aberration, coma, and astigmatism. It was assumed that these coefficients could be represented by an equation of the form for spherical aberration:

$$B = B_0 + \sum_{i=0}^{i=j} [B_{12_i}(k_{12} - 1)^i + B_{34_i}(k_{34} - 1)^i + B_{56_i}(k_{56} - 1)^i].$$

B_0 is the coefficient of the spherical contribution of the original lens, and k_{12} is the bend parameter for a forward bend at surfaces one and two. Since k = 1 represents no change to a system, the form $k_{ab} - 1$ was assumed to be the variable. Now the functions such as $B_{12_i}(k_{12} - 1)^i$ represent a change to the spherical contribution as a result of a forward bend at surfaces one and two. Program BREAK2 was changed to perform j bends at each of the three bend locations. It established a data file DELB, which contained the change of a contribution versus the value of $k_{ab} - 1$. Figure 17 shows diagrammatically these programs in relation to subsequent programs.

A General Electric system program POLFIT was used to fit these data to a least-squares polynomial. This provided the value of the coefficients B_{12_i}, B_{34_i}, B_{56_i}, F_{12_i}, ..., C_{56_i}. These coefficients along with the values for B_0, F_0, and C_0, from BREAK2 provided a system of three simultaneous nonlinear equations in three unknowns. Solving this system for zero would, in principle, yield the values for the bend parameter at these three locations, which would give zero third-order spherical aberration, coma, and astigmatism.

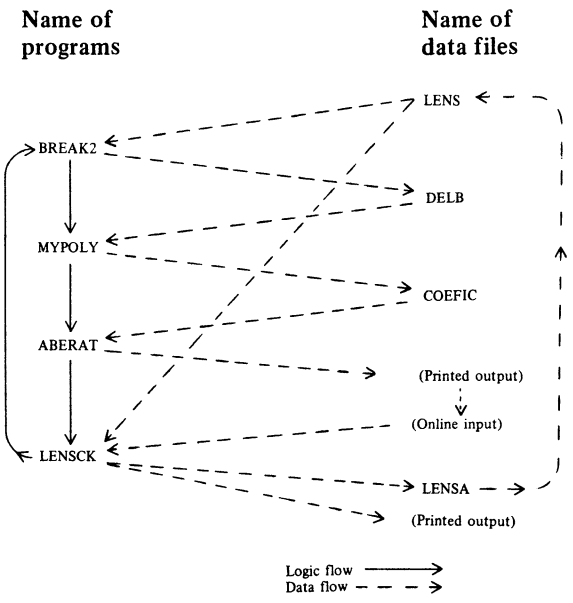

Figure 17. Flow diagram for correcting third-order spherical aberration, coma, and astigmatism.

To solve this system of equations, a second General Electric system program, SECANT, was used. I modified the program POLFIT (renamed MYPOLY) to read the data file DELB prepared by BREAK2. MYPOLY established a data file COEFIC, which contained the values of the coefficients for the system of three equations. A FORTRAN program ABERAT was written to formulate the system of three equations using the data in COEFIC. It then called SECANT to solve the set of equations and to return the three values $(k_{12}-1)$, $(k_{34}-1)$, and $(k_{56}-1)$. The accuracy of this solution depended on the accuracy with which the polynomials actually represented the change in an aberration as a function of the bend parameter. To check this, a modified version of BREAK2 (LENSCK) performed the three specified bends and calculated the actual Seidel coefficients for the new lens.

To summarize how the whole routine was used: First, a data file LENS was established that was the description of a lens. The first number in the file was the number of surfaces in the lens. Then, following in sequence, was the curvature, thickness, refractive index, and dispersion of the first surface. This was repeated sequentially for the remaining surfaces. For the triplet used, I specified eight surfaces with the first being the entrance pupil and the last being the image plane. The stop plane was omitted since its curvature obviously could not be varied and would lead to confusion on some results.

With this file specified, the program BREAK2 was run. It would ask the operator for the number of bends to be made and the value of bend parameters desired. A maximum of ten bends at each location could be made. Next, MYPOLY was run. It would ask the operator for the degree of the polynomial to which the data in DELB was to be fitted. Any degree less than the number of bends made could be specified, but in practice I always used the maximum degree. This prepared file COEFIC, which was used by running ABERAT. When LENSCK was run, it asked for the three values that represented the solution from ABERAT. LENSCK also utilized the data file LENS as a starting point and calculated a new lens that was entered in data file LENSA. It calculated the new actual aberration coefficients and printed them as output. With this setup,

it was possible to perform an interative process. File LENSA could be substituted for LENS in BREAK2, and the whole process could be repeated with LENSCK starting from LENSA and establishing another file LENSB.

This procedure, without use of the iteration technique, was used to find out what degree of polynomial was required to represent the change of an aberration coefficient as a function of the bend parameter and to find out what range of bends was required for this polynomial approximation. Eight runs were made varying the number of bends from three to ten. In each case the maximum degree of fit was specified in MYPOLY, and the trial values of k were varied roughly from 0.5 to 2.0 (Table 1). It was found that as the degree of approximation was increased, there was always a decrease in the sum of the absolute value of the aberrations. Making three bends and letting a second-degree polynomial represent the change of a contribution as a function of the bending resulted in a decrease of the contribution by a factor of two. Making ten bends and fitting to a ninth-degree polynomial resulted in a decrease by a factor of ten thousand.

Next, the trial values of k were reduced to the range 0.75 to 1.5 (Table 2) and then to the range 0.9 to 1.2 (Table 3). In these last two cycles, a maximum of eight bends was made for each range of k. It was noted that as the range of k values was decreased, the process seemed to converge a little more rapidly but still to the same solution.

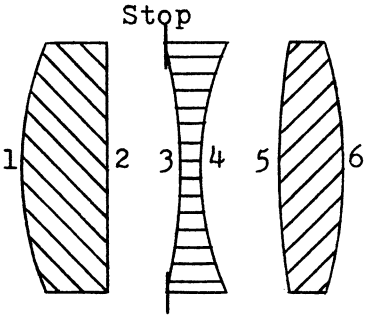

LENS SPECIFICATION

Surface	Radius of curvature (mm)	Thickness (mm)*
1	37.1	9.933
2	∞	6.507
Stop		1.8
3	-59.9	1.463
4	34.8	8.782
5	86.5	7.533
6	-50.9	80.767
Image plane		

*Of medium following the surface

Figure 18. Triplet corrected for third-order spherical aberration, coma, and astigmatism. This lens is the result of forward bends at surfaces 1 and 2 (k=1.342), surfaces 3 and 4 (k=0.9472), and surfaces 5 and 6 (k=1.177) of the original triplet (Fig. 3), which results in zero third-order spherical aberration, coma, and astigmatism.

With each range, the solution that most nearly made B, F, and C equal zero was $k_{12} = 1.342$, $k_{34} = 0.9472$, and $k_{56} = 1.177$ (Fig. 18). The reason for the two smaller ranges of bends converging more rapidly was probably because the actual final solution lay closer to these regions. Still, a high degree of approximation was required to obtain the solution. It may be that a power series is not well suited for the approximation.

Finally, a linear approximation was made for the change of the contribution as a function of k. The data points used were for k = 1.0 and k = 1.01. The iterative technique was used. By the end of the third iteration, the procedure had arrived at the same solution as the previous higher-degree noniterative procedure. It would seem that this would be much faster because it was so much simpler. However, in actual computer time used, the three simple iterations took twice as long as the ninth-degree approximation run. Of course, programs could be made much simpler if only linear approximations were to be made. The total time for the iterative technique might then be shorter than for a one-step technique; however, this was not determined. The important conclusion seems to be that it is possible, with a sufficiently high degree of approximation, to arrive at the solution in one step.

Table 1. Reduction of aberration coefficients versus number of trial bends for k = 0.5 to 2.0.

	Solution (bend parameter)			Reduced aberration coefficients		
No. of bends	Surfaces 1 & 2	Surfaces 3 & 4	Surfaces 5 & 6	B	F	C
				-0.0474*	0.00995*	0.0639*
3	0.23071	1.01378	1.04772	-0.0298	-0.00293	0.00425
4	0.69852	0.98753	1.10414	-0.0143	-0.00522	-0.000343
5	1.69911	0.92597	1.21993	0.00724	0.00298	0.000687
6	1.41708	0.94270	1.18587	0.00155	0.000606	0.000123
7	1.32099	0.94845	1.17468	-0.000426	-0.000174	-0.0000560
8	1.33570	0.94757	1.17635	-0.000128	-0.0000495	-0.0000154
9	1.34507	0.94702	1.17740	0.0000611	0.0000243	0.0000118
10	1.34189	0.94721	1.17704	-0.00000484	0.00000141	0.00000576

*Initial values.

Table 2. Reduction of aberration coefficients versus number of trial bends for k = 0.75 to 1.5.

	Solution (bend parameter)			Reduced aberration coefficients		
No. of bends	Surfaces 1 & 2	Surfaces 3 & 4	Surfaces 5 & 6	B	F	C
				-0.0474*	0.00995*	0.0639*
3	0.68128	0.98892	1.09693	-0.0162	-0.00402	0.00220
4	1.22458	0.95471	1.16323	-0.00242	-0.00126	-0.000146
5	1.35949	0.94614	1.17912	0.000363	0.000149	0.0000248
6	1.34216	0.94719	1.17709	0.00000387	0.00000221	-0.000000482
7	1.34261	0.94716	1.17713	0.0000124	0.00000567	0.00000208
8	1.34205	0.94720	1.17707	0.000000156	-0.0000000764	-0.000000335

*Initial values.

Table 3. Reduction of aberration coefficients versus number of trail bends for k = 0.9 to 1.2.

	Solution (bend parameter)			Reduced aberration coefficients		
No. of bends	Surfaces 1 & 2	Surfaces 3 & 4	Surfaces 5 & 6	B	F	C
				-0.0474*	-0.00995*	0.0639*
3	1.24317	0.95351	1.16472	-0.00220	-0.000864	0.000182
4	1.34008	0.94735	1.17687	-0.0000256	-0.0000587	-0.0000219
5	1.34036	0.94730	1.17687	-0.0000339	-0.0000124	-0.00000265
6	1.34215	0.94720	1.17708	0.00000291	-0.000000281	0.00000185
7	1.34205	0.94721	1.17706	0.000000749	-0.00000385	0.00000296
8	1.34131	0.94721	1.17707	-0.00000375	0.00000734	-0.0000297

*Initial values.

CHAPTER 5

CONCLUSIONS

The basic premise of generalized bending, holding first-order properties constant except at a small selected region, suggests its use to control third-order aberrations. It has been shown that this is possible, and that selected aberrations can be effectively reduced to zero. Although it requires a fifth-degree polynomial or more, it is possible to express the change of an aberration coefficient as a function of a bending parameter. This permits the simultaneous correction of several aberrations in one step. It is also possible to make a linear approximation of this change, but this requires several cycles to reduce the aberration coefficient to a desired value. The fact that a high degree of approximation is required suggests that a polynomial other than a power series would fit this change better. In principle one should be able to express the contribution of a surface as an exact function of the bend parameter. This would involve writing the aberration contribution of a surface in terms of the original lens parameters, original paraxial ray trace values, and bend equations, including the bend parameter.

The most serious drawback of using generalized bending to correct third-order aberration coefficients is that many lens variables are used rapidly. One independent generalized bend ties up four lens parameters. In the case of the triplet, only spherical aberration, coma, astigmatism, and focal length were controlled, while distortion, field curvature, and color were uncontrolled. Therefore, generalized bending is of limited value for the correction of simple systems. On the other hand, it would be very useful in more complex systems to control first- and third-order properties.

The insight that is available to the designer as a result of ray fan plots as a function of various generalized bends seems to be considerable. The possibility of using various nodes at various locations in the aperture for control should be investigated further. The various plots suggest elements that control coma, or field curvature, or distortion. Although an exhaustive series of plots was made in this investigation, it would appear that a sketchier series of fans would provide the information necessary for making corrections.

Furthermore, the ray fan plots give us a good appreciation of the magnitude of the bend parameter required to effect a significant change in the lens' quality. A range of bends from $k = 0.8$ to $k = 1.25$ seems to be more than adequate to show what an element is doing. The thickness between the two surfaces being bent is important to consider for the possibility of Q_1 becoming zero and to prevent a negative thickness from resulting. If this thickness is relatively large, it must be watched much more closely.

ACKNOWLEDGMENTS

The author would like to express his sincere appreciation for the encouragement and forbearance of his thesis advisor, Dr. Orestes N. Stavroudis, during the preparation of this report.

The author also would like to extend his appreciation to Dr. Dean B. McKenney for his assistance in debugging the computer programs written for use in this report.

REFERENCES

Feder, D. P., 1951, "Optical calculations with automatic computing machinery," J. Opt. Soc. Am. 41(9):630-635.

Hopkins, R. E., 1962, "Method of lens design," Section 9 in *MIL-HDBK-141,* Defense Supply Agency, Washington, D.C.

Hopkins, R. E. and Hanau, R., 1962, Sections 5, 6, and 8 in *MIL-HDBK-141*, Defense Supply Agency, Washington, D.C.

Jenkins, F. A. and White, H. E., 1957, "Lens aberrations," Chapter 9 in *Fundamentals of Optics*, 3rd ed., McGraw-Hill Book Company, New York.

Merte, W. W., 1950, *The Zeiss Index of Photographic Lenses,* Vol. I, The Central Air Document Office (Army, Navy, Air Force), Wright-Patterson Air Force Base, Dayton, Ohio.

Sutton, L. E., 1963, "A method for localized variation of the paths of two paraxial rays," Appl. Opt. 2(12):1275-1280.

ksh